Trapped Field Characteristics and Fracture Behavior of REBaCuO Bulk Ring During Pulsed Field Magnetization

Hidehiko Mochizuki, Hiroyuki Fujishiro, Tomoyuki Naito, Yoshitaka Itoh, Yousuke Yanagi, and Takashi Nakamura

***Abstract*—We have performed pulsed field magnetization (PFM) for the GdBaCuO ring bulk (60 mm in outer diameter, 36 mm in inner diameter, and 17 mm in thickness) with an aluminum alloy bandage at 65 K. When a magnetic pulsed field over 3 T was applied, a fracture was confirmed in the bulk by the trapped field profile. Using a numerical simulation by a finite-element method, the trapped field and the hoop (σ_θ) and radial (σ_r) stresses were analyzed. A huge compressive stress concentrated at the inner peripheral edge of the ring bulk mainly by the thermal contraction. The additional compressive stress was applied by the flux-pinning-induced magnetostriction around the maximum field during PFM. The mechanical reinforcement in the inner periphery part of the ring bulk must be considered during PFM using a cylinder.**

***Index Terms*—Compressive stress, fracture behavior, pulsed field magnetization (PFM), REBaCuO bulk ring.**

I. Introduction

NUCLEAR magnetic resonance (NMR) spectrometer with high resolution is a powerful apparatus to analyze complex molecular structure or to develop new drugs. Recently, 1020 MHz (24.0 T) NMR spectrometer using novel and complex superconducting coils has been developed [1]. A compact and cryogen-free NMR spectrometer with a medium resolution of 200 MHz (4.7 T)—270 MHz (6.3 T) is also desired, because a large superconducting coil magnet system for NMR cooled by liquid helium is very expensive and occupies a wide space to realize the homogeneity of the magnetic field. REBaCuO superconducting bulk (RE: rare earth element and Y) has a promising potential as a quasi-permanent magnet, which can trap a high magnetic field over 17 T by the reinforcement against the electromagnetic force [2], [3]. One of the practical applications using the bulk magnet is a compact cryogen-free NMR magnet. Nakamura *et al.* developed REBaCuO superconducting bulk magnet for the 2.89 T (123 MHz) NMR spectrometer using six annular REBaCuO bulk rings, which were magnetized by field cooled magnetization (FCM) using a superconducting coil magnet [4]. The NMR spectra of ethanol with a full width at half of the maximum (FWHM) of 0.1 ppm (21 Hz) were observed with a 1.3 mm diameter and 4 mm length using a multichannel shim coil [5]. The magnetic resonance imaging (MRI) was also investigated using annular EuBaCuO bulks [5], [6]. A new technique to realize the field homogeneity in the cylindrical bulk has been proposed and confirmed by the insertion of the cylinder wrapped by high-J_c superconducting tapes [7]. We confirmed the insertion effect using a numerical simulation [8].

Pulsed field magnetization (PFM) is a promising technique to magnetize the superconducting bulk, because of the compact and inexpensive experimental setup with no use of superconducting coil magnet. However, the trapped field B_z by PFM is lower than that by FCM because of a large temperature rise caused by the dynamical motion of the magnetic flux. We have studied the PFM technique mainly for the disk shaped bulk experimentally and numerically to enhance the trapped field B_z [9], [10]. If the trapped field strength and the field homogeneity are fairly enhanced in the REBaCuO cylindrical bulk magnetized by PFM, the magnetizing technique to realize the NMR bulk magnet might be replaced from FCM to PFM.

During the magnetizing process for superconducting bulks, the mechanical strength must be considered to avoid their fracture, because a huge flux pinning induced magnetostriction is exerted on the bulk. For the FCM process, both hoop and radial stresses are experienced in the bulk. The disk bulk is usually reinforced by fitted metal ring or a glass fiber to prevent the fracture from expansive stress [2], [3]. For the PFM process, a compressive stress is also applied at the ascending stage of PFM. REBaCuO bulk is a brittle ceramic material, and has a low mechanical strength of 30–100 MPa [11], [12]. Ren *et al.* reported that cracking is more likely during activation and most probable at the center of the disk bulk with the cracks running outward for FCM [13]. Johansen *et al.* calculated the hoop and radial stresses during FCM and zero-field cooled magnetization (ZFCM) [14], [15]. These papers were based on the Bean's

Manuscript received October 16, 2015; accepted December 15, 2015. Date of publication December 30, 2015; date of current version January 15, 2016. This work was supported in part by the project "Development of System and Technology for Advanced Measurement and Analysis" of the Japan Science and Technology Agency (JST) and by the Japan Society for the Promotion of Science (JSPS) under KAKENHI Grant 15K04646.

H. Mochizuki, H. Fujishiro, and T. Naito are with the Faculty of Engineering, Iwate University, Morioka 020-8551, Japan (e-mail: t2214035@iwate-u.ac.jp; fujishiro@iwate-u.ac.jp; tnaito@iwate-u.ac.jp).

Y. Itoh and Y. Yanagi are with the IMRA Material R&D Company Ltd., Kariya 448-0032, Japan (e-mail: y-itoh@ai-i.aisin.co.jp; yanagi@ai-i.aisin.co.jp).

T. Nakamura is with RIKEN, Wako 351-0198, Japan (e-mail: takashi.nakamura@riken.jp).

Color versions of one or more of the figures in this paper are available online at http://ieeexplore.ieee.org.

Digital Object Identifier 10.1109/TASC.2015.2513415

model for the c-axis oriented long superconducting cylinder. The increase in the mechanical strength of the bulk by adding Ag and the mechanical reinforcement is the most important issue.

In this paper, we performed PFM experiments for the GdBaCuO ring bulk to apply to NMR spectrometer. Unfortunately, the ring bulk was broken during PFM process. We analyzed the time dependence of the hoop and radial stresses in the ring bulk using a finite element method (FEM) and discussed the reason of the fracture occurrence and the method to prevent it.

II. Experimental Procedure

Ag-doped GdBaCuO ring bulk (60 mm in outer diameter, 36 mm in inner diameter and 17 mm in height) was used, which was fabricated by the modified quench and melt growth (QMG) method. The ring bulk was glued in aluminum alloy ring (60.1 mm in inner diameter and 5 mm in thickness) using epoxy resin to prevent the mechanical fracture against the expansive hoop strain. The ring bulk was mounted on the cold stage of the Gifford McMahon (GM) cycle helium refrigerator and the initial temperature T_s was set to 65 K. Magnetizing solenoid copper coil dipped in the liquid nitrogen was placed outside the vacuum chamber. The magnetic pulse B_{ex} $(= 2.5 \sim 3.1$ T) with a rise time of 13 ms was applied to the ring bulk. A local magnetic field $B_L^C(t)$ was monitored by axial-type hall sensor (BHA 921; F. W. Bell) at the center of the hole using digital oscilloscope. Two-dimensional trapped field profile B_z was mapped 1 mm above the bulk surface using the same hall sensor. The detailed experimental procedure is described elsewhere [9], [10].

III. Modeling of Numerical Simulation

Based on the experimental setup of PFM, we proposed the following framework of numerical simulation. An infinite long cylindrical superconducting bulk (60 mm in outer diameter and 36 mm in inner diameter) was mounted in aluminum alloy cylinder (60.1 mm in inner diameter and 5 mm in thickness) using epoxy resin. The critical current density J_c of the bulk was supposed to be 2.25×10^8 A/m^2, which was a typical J_c value at 65 K for the present bulk and was supposed to be independent of temperature and magnetic field according to the Bean's critical state model. In this case, a disk bulk with $r = 30$ mm in radius is fully magnetized with $B^* = \mu_0 J_c r = 8.48$ T by FCM. In the simulation, the imaginary magnetic pulse was applied from 0 to B_{ex} by 10 steps at the ascending stage and then from B_{ex} to 0 by 10 steps at the descending stage using a pulse coil (100 mm in inner diameter). The compressive stress generated by the thermal contraction cooled from 300 K to 65 K was also calculated. The mechanical parameters (Young's modulus E, Poisson ratio γ, bulk modulus B and thermal expansion coefficient α) used in the elastic simulation are summarized in Table I. Commercial software, Photo-Eddy, combined with Photo-ELAS (Photon Ltd., Japan), was used for the analysis of the distributions of magnetic field, current density and elastic stress in the cylindrical bulk during PFM.

TABLE I
Mechanical Parameters Used in the Numerical Simulation

	E (Pa)	γ	B (Pa)	α (K^{-1})
ring bulk	1.0e11	0.33	1.0e11	5.2e-6
coil	1.0e11	0.30	1.0e11	1.0e-8
Al alloy ring	7.8e10	0.34	7.8e10	1.48e-5
epoxy resin	3.0e9	0.37	3.0e9	2.4e-5
air	1.0e0	0.10	1.0e0	1.0e-8

(E: Young's modulus, γ: Poisson ratio, B: bulk modulus, α: thermal expansion coefficient)

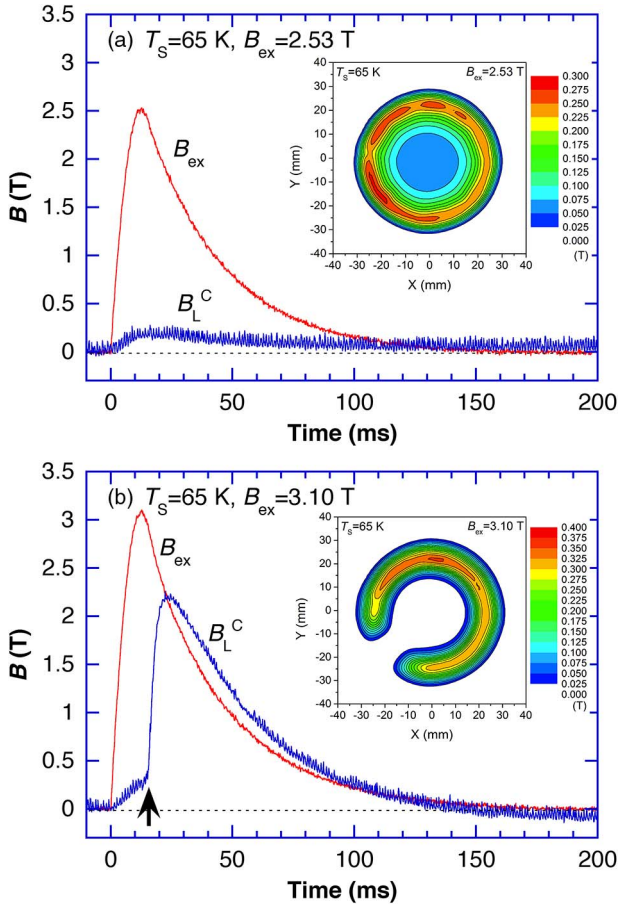

Fig. 1. Time dependence of the local field B_L^C and the applied pulsed field B_{ex} at the center of the hole for (a) $B_{ex} = 2.53$ T and (b) 3.10 T at 65 K. The thick arrow shows the estimated position, at which the ring bulk was broken.

IV. Experimental Results

Fig. 1 shows the time dependence of the local field $B_L^C(t)$ and the applied pulsed field $B_{ex}(t)$ for $B_{ex} = 2.53$ T and 3.10 T at 65 K. For $B_{ex} = 2.53$ T, the magnetic flux can hardly penetrate into the ring bulk because of a pulsed field too low to overcome the magnetic shielding. The inset shows the trapped field profile, in which a small amount of magnetic flux was trapped concentrically at the bulk periphery. On the other hand, for $B_{ex} = 3.10T$, magnetic flux intruded abruptly at the central position from $t = 15$ ms. B_L^C reaches a maximum at $t = 24$ ms and decreased with increasing time. However, the trapped field B_z was hardly generated and showed a slightly negative value

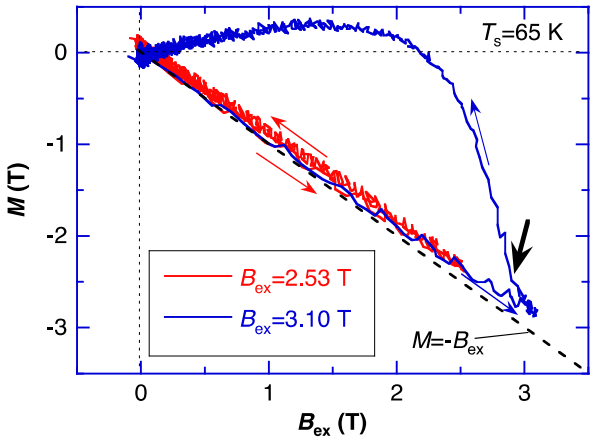

Fig. 2. Magnetization curve for each applied field B_{ex}, which was calculated by $M = B_{\mathrm{L}}^{\mathrm{C}}(t) - B_{\mathrm{ex}}(t)$ using Fig. 1. The thick arrow shows the estimated position, at which the ring bulk was broken.

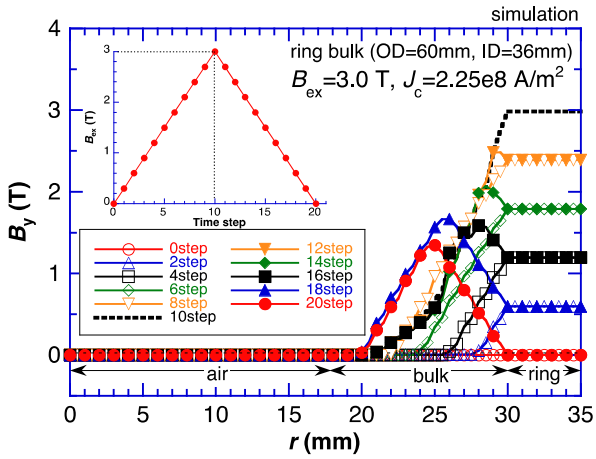

Fig. 3. Time step dependence of the profile of the local field B_{y} after applying the magnetic pulsed field of $B_{\mathrm{ex}} = 3.0$ T.

at the center of the hole. The trapped field profile shown in Fig. 1(b) suggested a crack creation at the lower left position in ring bulk. We conceived that the bulk was broken during PFM and the superconducting current circumvented by the crack, although we were not able to confirm any cracks on the bulk surface using an optical microscope. For the descending stage of PFM, an expansive stress is applied to the ring bulk with an aluminum alloy bandage, which is the same situation for the FCM process. The aluminum alloy bandage is effective to prevent the mechanical fracture from the expansive force. However, for the ascending stage of PFM, a compressive force was applied to the ring bulk without any reinforcement inside the ring bulk and, as a result, the ring bulk might be broken.

Fig. 2 presents the magnetization curve for each B_{ex}, which was calculated by $M = B_{\mathrm{L}}^{\mathrm{C}}(t) - B_{\mathrm{ex}}(t)$ using Fig. 1. In the ascending stage of $B_{\mathrm{ex}}(t)$, the magnetic flux can hardly penetrate into the bulk center and the M value is nearly equal to the negative applied field, $(M = -B_{\mathrm{ex}})$. A wide hysteresis loop in the M vs. B_{ex} curve and a slightly negative final M value with increasing time can be seen. We cannot precisely conclude when the crack was created from Figs. 1 and 2, but the time to take place the fracture is predicted to be just after the peak of $B_{\mathrm{ex}}(t)$ $(t = 15$ ms) as shown by the thick arrow in the figures.

V. Results of Numerical Simulation and Discussion

A. Hoop and Radial Stresses by the Electromagnetic Force

Fig. 3 shows the time step dependence of the profile of the local field B_{y} for $B_{\mathrm{ex}} = 3.0$ T. The inset shows the time step of B_{ex}. The magnetic flux intruded and was trapped only at the bulk periphery because of lower B_{ex} than B^*, which fairly represents the Bean's critical state model.

Fig. 4(a) and (b) present the time step dependence of the profile of the hoop stress (σ_θ) and the radial stress (σ_{r}) for $B_{\mathrm{ex}} = 3.0$ T. In Fig. 4(a), the compressive hoop stress (σ_θ) increases with increasing strength of the pulsed field and takes a maximum of -7.21 MPa at the maximum $B_{\mathrm{ex}} = 3$ T and then decreases. After the 14 steps, which is lower than 1.8 T,

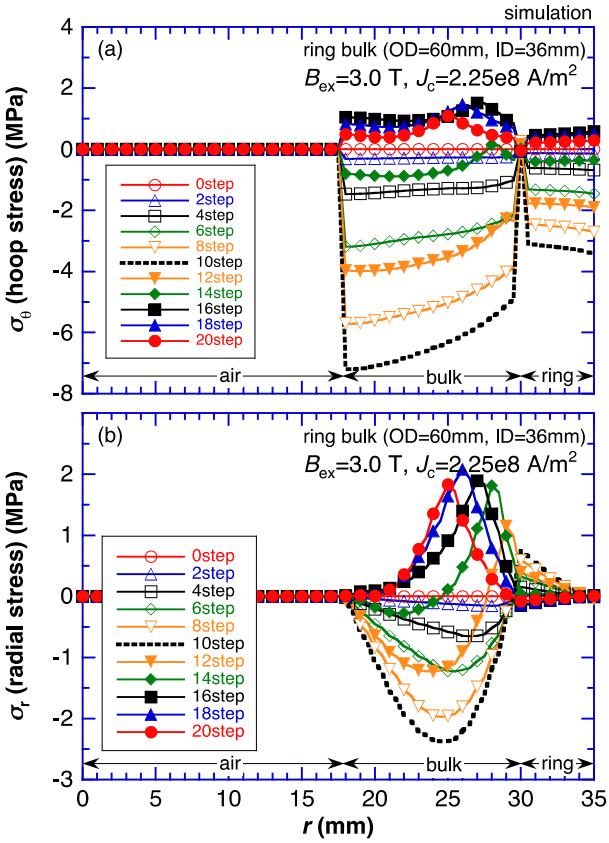

Fig. 4. Profile of the (a) hoop stress (σ_θ) and (b) radial stress (σ_{r}) in the bulk during PFM, as a function of time step of $B_{\mathrm{ex}} = 3.0$ T.

the hoop stress changes to the positive value. It should be noted that the maximum compressive hoop stress takes place at the inner periphery edge and at the maximum applied field. The dip of the hoop stress at $r = 30$ mm results from the existence of the epoxy resin with low Young's modulus. In Fig. 4(b), the compressive radial stress (σ_{r}) increases with increasing strength of the pulsed field and takes a maximum at the maximum $B_{\mathrm{ex}} = 3$ T and then decreases. At the descending stage, the radial stress changes to the positive value.

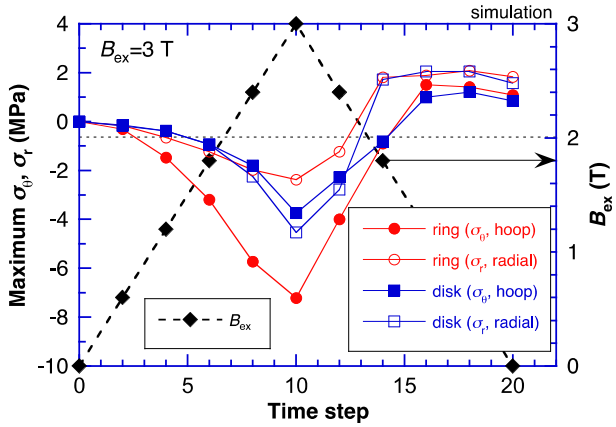

Fig. 5. Time step dependence of the maximum σ_θ and σ_r values for the ring bulk and the disk bulk during PFM of 3 T.

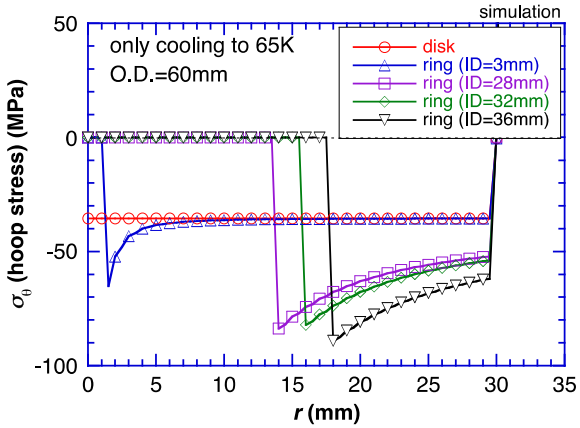

Fig. 6. Profile of the hoop stress (σ_θ) for the disk bulk and the cylindrical bulks with various inner diameters only by the cooling to 65 K.

The maximum σ_r value is smaller than σ_θ and the maximum position of the σ_r value is not situated at the inner periphery edge, but in the bulk.

Fig. 5 summarizes the time step dependence of the maximum σ_θ and σ_r values shown in Fig. 4. The similar values for the disk bulk with the same outer diameter $(\mathrm{OD} = 60\ \mathrm{mm})$ are also shown. The maximum compressive σ_θ and σ_r values for each bulk attain at the maximum pulsed field. The maximum compressive σ_θ of the cylindrical bulk is about twice as large as that of the disk bulk.

B. Thermal Contraction Down to 65 K

Fig. 6 shows the profile of the hoop stress (σ_θ) for the disk bulk and the cylindrical bulks with various inner diameters by the only cooling to 65 K. For the disk bulk, the compressive hoop stress is -35.4 MPa, which is independent of the distance from the center. For the cylindrical bulk, the compressive hoop stress is enhanced at the inner periphery edge of the cylinder, which increases with increasing inner diameter. The maximum compressive hoop stress of the cylinder 36 mm in inner diameter is -89.1 MPa, which is about twice larger than

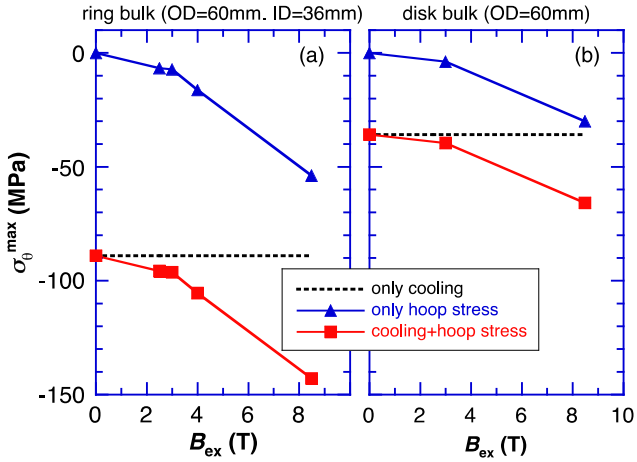

Fig. 7. Applied pulsed field dependence of the maximum hoop stress (σ_θ) at 65 K for the (a) cylindrical bulk (OD = 60 mm, ID = 36 mm) and (b) disk bulk (OD = 60 mm).

that of the disk bulk. The compressive hoop stress by the thermal contraction is about ten times larger than that by the electromagnetic force shown in Fig. 4(a).

In the actual PFM experiments, the stress by the flux pinning induced magnetostriction is applied to the bulk cooled down to 65 K. In this sense, the stress by the flux pinning induced magnetostriction was added to that by the thermal contraction. Fig. 7(a) shows the applied pulsed field dependence of the maximum hoop stress (σ_θ) of the cylindrical bulk $(\mathrm{ID} = 36\ \mathrm{mm})$ at 65 K. The σ_θ values only by the cooling and only by the electromagnetic force are also shown. The hoop stress without cooling increases with increasing B_{ex}. The maximum compressive hoop stress at 65 K, which is the sum of both contributions, exceeds -95 MPa for $B_{ex} = 3.0$ T, which suggests that the value may be larger than that of the mechanical strength of the REBaCuO bulk ranging 30–100 MPa [11], [12]. Fig. 7(b) shows the same relation for the disk bulk for comparison. The hoop stresses for the disk bulk by both thermal contraction and electromagnetic force is small, compared to those for the ring bulk $(\mathrm{ID} = 36\ \mathrm{mm})$. In order to avoid the mechanical fracture of the cylindrical bulk during PFM, the reinforcement of the inner periphery part must be considered using, for example, a ring material with negative thermal expansion coefficient and with higher mechanical strength.

VI. Conclusion

Pulsed field magnetization (PFM) for the GdBaCuO bulk ring with an aluminum alloy bandage has been performed at 65 K. A mechanical fracture was confirmed just after the magnetic pulse takes a maximum of 3 T. Using the numerical simulation, it was confirmed that a huge compressive stress was concentrated at the inner peripheral edge of the ring bulk just after the maximum magnetic pulse in PFM, together with the thermal contraction cooling down to 65 K. The reinforcement of the inner periphery part of the cylindrical bulk must be considered.

REFERENCES

[1] K. Hashi *et al.*, "Achievement of 1020 MHz NMR," *J. Magn. Reson.*, vol. 256, pp. 30–33, 2015.

[2] M. Tomita and M. Murakami, "High-temperature superconductor bulk magnets that can trap magnetic fields of over 17 tesla at 29 K," *Nature*, vol. 421, pp. 517–520, 2003.

[3] J. H. Durell *et al.*, "A trapped field of 17.6 T in melt-processed, bulk Gd–Ba–Cu–O reinforced with shrink-fit steel," *Supercond. Sci. Technol.*, vol. 27, 2014, Art. ID 082001.

[4] T. Nakamura, Y. Itoh, M. Yoshikawa, T. Oka, and J. Uzawa, "Development of a superconducting magnet for nuclear magnetic resonance using bulk high-temperature superconducting materials," *Concepts Magn. Reson.*, vol. 31B, pp. 65–69, 2007.

[5] T. Nakamura *et al.*, "Development of a superconducting bulk magnet for NMR and MRI," *J. Mag. Reson.*, vol. 259, pp. 68–75, 2015.

[6] K. Ogawa, T. Nakamura, Y. Terada, K. Kosuke, and T. Haishi, "Development of a magnetic resonance microscope using high T_c bulk superconducting magnet," *Appl. Phys. Lett.*, vol. 98, 2011, Art. ID 234101.

[7] Y. Itoh, Y. Yanagi, and M. Yoshikawa, Jpn. Patent 2014-127301, Jun. 20, 2014.

[8] H. Fujishiro, Y. Itoh, Y. Yanagi, and T. Nakamura, "Drastic improvement of the trapped field homogeneity in a superconducting hollow bulk by the insertion of a high-J_c superconducting cylinder for NMR bulk magnets," *Supercond. Sci. Technol.*, vol. 28, 2015, Art. ID 095018.

[9] M. D. Ainslie *et al.*, "Modelling and comparison of trapped fields in (RE)BCO bulk superconductors for activation using pulsed field magnetization," *Supercond. Sci. Technol.*, vol. 27, 2014, Art. ID 065008.

[10] H. Fujishiro and T. Naito, "Simulation of temperature and magnetic field distribution in superconducting bulk during pulsed field magnetization," *Supercond. Sci. Technol.*, vol. 23, 2010, Art. ID 105021.

[11] D. Lee and K. Salama, "Enhancements in current density and mechanical properties of Y-Ba-Cu-O/Ag composites," *Jpn. J. Appl. Phys.*, vol. 29, pp. L2017–2019, 1990.

[12] H. Fujimoto and A. Murakami, "Mechanical properties of Gd123 superconducting bulks at 77 K," *Supercond. Sci. Technol.*, vol. 25, 2012, Art. ID 054017.

[13] Y. Ren, R. Weinstein, J. Liu, R. P. Sawh, and C. Foster, "Damage caused by magnetic pressure at high trapped field in quasi-permanent magnets composed of melt-textured Y–Ba–Cu–O superconductor," *Phys. C*, vol. 251, pp. 15–26, 1995.

[14] T. H. Johansen, "Flux-pinning-induced stress and strain in superconductors: Case of a long circular cylinder," *Phys. Rev. B*, vol. 60, pp. 9690–9703, 1999.

[15] T. H. Johansen, C. Wang, Q. Y. Chen, and W.-K. Chu, "Enhancement of tensile stress near a hole in superconducting trapped-field magnets," *J. Appl. Phys.* vol. 88, pp. 2730–2733, 2000.